CHAINED COMPUTATIONS USING AN UNSTEADY 3D APPROACH FOR THE DETERMINATION OF THERMAL FATIGUE IN A T-JUNCTION OF A PWR NUCLEAR PLANT

THOMAS PASUTTO, CHRISTOPHE PÉNIGUEL and MARC SAKIZ*
EDF R&D
Fluide Mechanics and Heat Transfer
6, quai Watier, 78401, Chatou, Franc
*Corresponding author. E-mail : marc.sakiz@edf.fr

Received February 6, 2006

Thermal fatigue of the coolant circuits of PWR plants is a major issue for nuclear safety. The problem is especially accute in mixing zones, like T-junctions, where large differences in water temperature between the two inlets and high levels of turbulence can lead to large temperature fluctuations at the wall. Until recently, studies on the matter had been tackled at EDF using steady methods: the fluid flow was solved with a CFD code using an averaged turbulence model, which led to the knowledge of the mean temperature and temperature variance at each point of the wall. But, being based on averaged quantities, this method could not reproduce the unsteady and 3D effects of the problem, like phase lag in temperature oscillations between two points, which can generate important stresses. Benefiting from advances in computer power and turbulence modelling, a new methodology is now applied, that allows to take these effects into account. The CFD tool *Code_Saturne*, developped at EDF, is used to solve the fluid flow using an unsteady L.E.S. approach. It is coupled with the thermal code Syrthes, which propagates the temperature fluctuations into the wall thickness. The instantaneous temperature field inside the wall can then be extracted and used for structure mechanics computations (mainly with EDF thermomechanics tool *Code_Aster*).

The purpose of this paper is to present the application of this methodology to the simulation of a straight T-junction mock-up, similar to the Residual Heat Remover (RHR) junction found in N4 type PWR nuclear plants, and designed to study thermal striping and cracks propagation. The results are generally in good agreement with the measurements; yet, in certain areas of the flow, progress is still needed in L.E.S. modelling and in the treatment of instantaneous heat transfer at the wall.

KEYWORDS : CFD, Code_Saturne, Syrthes, LES, Thermal Fatigue, Nuclear Power Plant, RHR

1. INTRODUCTION

Thermal fatigue of the coolant systems of PWR plants is a major issue for nuclear safety. The problem is especially accute in mixing zones, like T-junctions, where a large difference of water temperature between the two entry branches and the high level of turbulence can lead to large temperature fluctuations at the wall. Civaux N4 class reactor was shut down in may 1998 following a leak of primary coolant from a pipe in the Residual Heat Removal (RHR) system. Cracks have been discovered in the elbow following the T-junction, that were clearly the result of thermal fatigue. Since then, the RHR pipeworks have been redesigned at all four EDF's N4 units and a large research program has been launched to address this issue. One of its contents is a cooperation with CEA and Framatome ANP on the study of a real-scale model of straight T-junction, based on the RHR junction geometry, on which fine near-wall and in-wall temperature measurements are performed. The aim of this model is to get a better understanding of the thermal loads seen by the structure in such situation and to evaluate the capacity of numerical simulation to reproduce it. The present paper deals with this last aspect. In order to capture the physics properly, instantaneous thermohydraulic phenomena, thermal coupling between the fluid and the solid, as well as the thermal conduction inside the wall have to be accounted for. These aspects are described in detail in the present paper. Eventually, the 3D instantaneous solid temperature fields obtained by simulation are used to compute the resulting mechanical stresses [1]. But this last aspect is beyond the scope of this paper.

2. NUMERICAL APPROACH OF INTANTANEOUS THERMOHYDRAULIC PHENOMENA

The characteristics of the flows in mixing zones usually involve a high level of turbulence. Hence, Direct Numerical

Simulation is totally out of reach of even the most powerful computers. On the other hand, Reynolds Averaged Navier Stokes models (like k-ε or more advanced models) can deal with such flows rather easely. Yet, they sometimes lack accuracy in specific complex areas of the flow, and most of all they can only yield mean or low order averaged quantities, thereby overlooking any high frequency instantaneous aspects, which are yet essential in thermal fatigue studies. In the last few years, the growing of computer capacity has made mixing zones configuration accessible to a third and intermediate technique : Large Eddy Simulation. In LES, only the smaller scales of turbulence are modelled, whereas the large energy carrying structures are computed directly. Thus, LES provides 3D time dependent solutions, on which any kind of signal processing can be done, at much higher Reynolds numbers than DNS.

2.1 The CFD Tool Code_Saturne

The EDF finite volume CFD code, *Code_Saturne*, is used to solve Navier-Stokes equations on unstructured meshes. The flow is assumed incompressible and Newtonian and the density is only a function of temperature. Using LES, the filtered Navier-Stokes equations can be written as follows (the filtering operator is omitted for clarity), together with the equation for the temperature.

$$\frac{\partial \rho}{\partial t} + \frac{\partial \rho U_j}{\partial x_j} = 0 \tag{1}$$

$$\rho \frac{\partial U_i}{\partial t} + \rho U_j \frac{\partial U_i}{\partial x_j} = -\frac{\partial p^*}{\partial x_i} + \frac{\partial}{\partial x_j}\left[\mu_e\left(\frac{\partial U_i}{\partial x_j} + \frac{\partial U_j}{\partial x_i}\right)\right] - \frac{2}{3}\frac{\partial}{\partial x_i}\left(\mu_e \frac{\partial U_j}{\partial x_j}\right) + (\rho - \rho_0) g_i \tag{2}$$

$$\rho \frac{\partial T}{\partial t} + \rho U_j \frac{\partial T}{\partial x_j} = \frac{\partial}{\partial x_j}\left[\left(\frac{\lambda}{Cp} + \frac{\mu_t}{\sigma}\right)\frac{\partial T}{\partial x_j}\right] \tag{3}$$

In these equations, U_i are the filtered components of the velocity, p* stands for the pressure (minus the reference hydrostatic pressure), μ_e represents $\mu + \mu_t$ where μ and μ_t are respectively the molecular and subgrid-scale viscosities. T is the temperature, λ, Cp and σ respectively the fluid conductivity, specific heat and turbulent Prandtl number. It should be noted that in k-ε approaches, the turbulent viscosity models the turbulent effects on the whole energy spectrum, whereas in LES the subgrid viscosity only represents the small scale structures (high frequencies). In our computations, both a Smagorinsky model [2] and a more complex dynamic model [3] have been used to calculate the sub-grid viscosity. Concerning the near-wall modelling, our computations rely on a regular wall function. More details on LES in Code_Saturne can be found in [4], [5] and [6].

Before taking on the study presented here, *Code_Saturne* has been tested on a large number of academic and industrial validation cases (homogeneous turbulence, channel flows, tube bundles, T-junction, coaxial jet, ...).

2.2 Numerical Technique Used for Solving the Fluid Equations

In the collocated finite volume approach used in *Code_Saturne*, all variables are located at the centres of gravity of the cells (which may take any shape). The momentum equations are solved by considering an explicit mass flux (the three components of the velocity are thus uncoupled). Velocity and pressure coupling is insured by a SIMPLEC prediction/correction method with outer-iterations [7]. The Poisson equation is solved with a conjugate gradient method. The collocated discretisation requires a Rhie and Chow interpolation in the correction step to avoid oscillatory solutions [8]. This interpolation has been used in the present application, although it doesn't seem essential for unstructured meshes. For L.E.S. calculations, second order schemes are used in space (fully centred scheme for the velocity components, centered scheme with slope test for the temperature) and time (Crank-Nicolson with linearised convection). A second order Adams-Bashforth method is used for the part of the diffusion involving the transposed velocity gradient, to keep the velocity components uncoupled.

2.3 The Solid Code Syrthes

The solid code Syrthes relies on a finite element technique to solve the following general heat equation where all properties can be time, space or temperature dependent.

$$\rho C_p \frac{\partial T}{\partial t} = \frac{\partial}{\partial x_j}\left(k_s \frac{\partial T}{\partial x_j}\right) + \Phi_v \tag{4}$$

T is the temperature, Φ_v a volumic source or sink, ρ and Cp, respectively the density and the specific heat. ks (a matrix when the material is anisotropic) designates the conductive behaviour of the medium. Radiation phenomena from wall to wall can also be taken into account. For optimisation reasons, only two kinds of elements have been retained (6 nodes triangles in 2D, 10 nodes tetrahedra in 3D). More details on the possibilities of the finite element code Syrthes can be found in [9]. Like *Code_Saturne*, Syrthes has been checked thoroughly against experimental and analytical test cases proving that it provides very accurate solutions in problems similar to the present one.

2.4 The Solid Code Coupling

At the interface, every time step, the thermal coupling is performed. Let Ts be the temperature of the solid node at the interface, and Tf the temperature of the corresponding first node in the fluid domain. At the beginning of time step (n), *Code_Saturne* receives from Syrthes the value of $Ts^{(n)}$ and uses it to calculate the exchange coefficient $h^{(n)}$, defining the heat flux at the wall by $\varphi = h(Ts-Tf)$ and sends its value to Syrthes. Then, the two codes work separately. *Code_Saturne* calculates $Tf^{(n+1)}$ implicitely considering the heat flux $\varphi^{(n+1)}=h^{(n)}(Ts^{(n)}-Tf^{(n+1)})$ whereas Syrthes calculates $Ts^{(n+1)}$, also implicitely, considering the flux $\varphi^{(n+1)}=h^{(n)}(Ts^{(n+1)}-Tf^{(n)})$. The system is then ready to perform the next time step.

3. CONFIGURATION AND SIMULATION PARAMETERS

3.1 Physical Parameters

The global geometry of the mock-up is shown on Figure 1. In this specific study, the horizontal hot branch and the vertical cold branch are set respectively at a temperature of 204°C and 41°C. The total flow rate is set to 260 m^3/h and the velocity ratio between the cold flow branch and the total flow rate is 20%. The physical properties of the fluid and the solid (density, viscosity, diffusivity, ...) are calculated using polynomial approximations that were defined by regressions over a sample of values taken from a in-house database, in the considered range of temperature.

3.2 Meshes

In order to solve the former equations numerically, the geometry has to be dicretised. Here the mesh generators GiBi and Ideas have been used. Two fluid meshes have been generated, containing roughly 500 000 and 1 000 000 hexaedric cells (cf. Figure 2). The solid mesh is presented in Figure 3. It contains 370 000 nodes and 260 000 tetraedra. Figure 4 presents a close view of the solid mesh to underline how fine the discretisation is, especially near the fluid/ solid interface. Previous mechanical studies have determined that an optimal spatial discretisation (for the mechanical stresses computation taking place afterwards) is of the order of 100 μm for the first element, i.e. the first solid node within the wall is only 50 μm away from the interface. The instantaneous temperature variation of the wall should therefore be well captured.

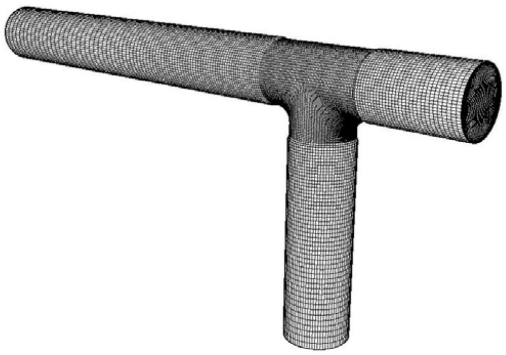

Fig. 2. Fluid Mesh (500 000 cells)

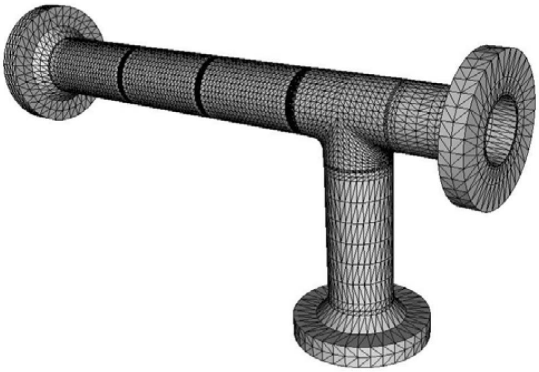

Fig. 3. Solid Mesh

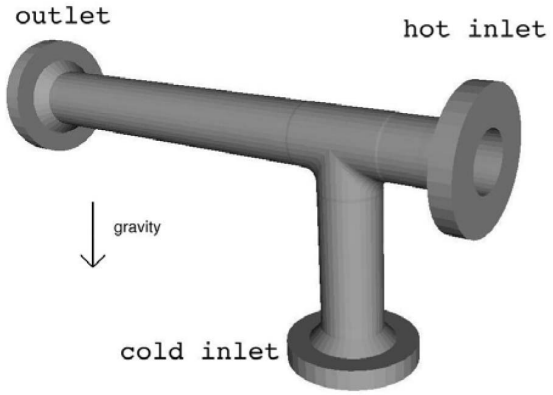

Fig. 1. General View of the Mock-up

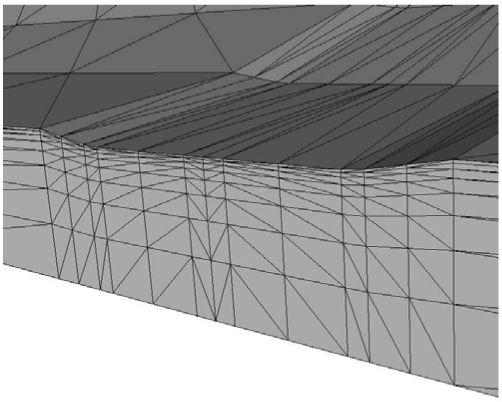

Fig. 4. Solid Mesh-Detail of the Discretisation at the Fluid Interface

3.3 Initial and Boundary Conditions

Initial conditions for the fluid flow present no problem, as they are evacuated very rapidely. It is however not the case for the solid, where at least 30 s of physical time would be necessary to wipe them off, which would be irrealistic to simulate with LES. Therefore a specific strategy is used. First the fluid flow is initialised over a few seconds, without any solid coupling (zero heat flux at the wall). Then, a semi-coupled calculation is started over a few seconds: the fluid temperature and exchange coefficient are calculated by *Code_Saturne* and send to Syrthes, but the effective boundary conditions for the fluid are still zero heat flux. At each point of the fluid/solid interface, the mean temperature and mean exchange coefficient are calculated. These values are then used as boundary conditions for a solid-only thermal computation with Syrthes over two hours of physical time. Hence the temperature field in the solid is in accordance with the fluid flow. After that, the proper fully coupled calculation is started.

Due to mesh limitations, the distance from the wall of the first calculation point in the fluid can be as large as 300 wall units for the coarser mesh, and 170 for the finer. Velocity and temperature boundary conditions therefore use usual wall functions. As for the entry conditions in the fluid, LES method requires to specify the instantaneous velocity. The mean part is estimated from the mean flow rate in each branch, and randow drawings are made at each entry point and at each time step, following a centred gaussian distribution, for the fluctuating part. The RMS value of the distribution is evaluated from the turbulence level expected in such a pipe flow. Other tests have been made using a more physical method of synthetic vortex creation, but it yields limited differences.

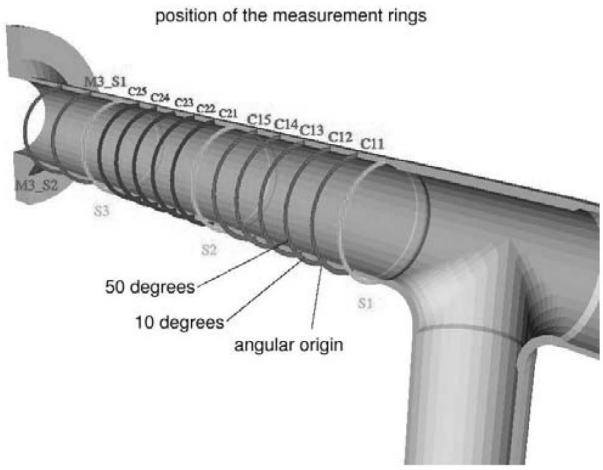

Fig. 5. Position of the Measurement Probes

4. COMPUTATIONAL RESULTS

These calculations give access to unsteady results on the entire solid and fluid domains. 10 s of physical time have been simulated for the Smagorinsky model on the coarser mesh, which corresponds to an already very large computational effort (around 1000 hours of CPU on a Fujitsu VPP5000 vector machine)[1]. Calculations with the dynamic model have been made on 32 parallel Alpha processors. 10 s of physical time have been simulated for a CPU time of 500 hours per processor. Results are mainly presented on different sections and the symmetry plane for which experimental measurements are available on site. These sections are pointed out in Figure 5. All thermal results are presented in non-dimensional variables; let Tcold and Thot be the cold and hot temperatures in the branches, the non-dimensional temperature and RMS temperature are calculated as:

$$T_{a\,dim} = \frac{T - T_{cold}}{T_{hot} - T_{cold}} \quad \text{which varies between 0 and 1}$$

$$\sigma_{Ta\,dim} = \frac{\sqrt{\overline{T'T'}}}{T_{hot} - T_{cold}}$$

Unless specified, the results presented in this paper correspond to the simulation with the coarser mesh and Smagorinsky model.

Figure 6 presents the instantaneous fluid velocity field in the symmetry plane at the physical time t=10 s. Figure 7 gives a snapshot of the fluid instantaneous temperature field. One may notice the strong irregularity of the stratification and the turbulent eddies created at the hot/cold interface and convected further away.

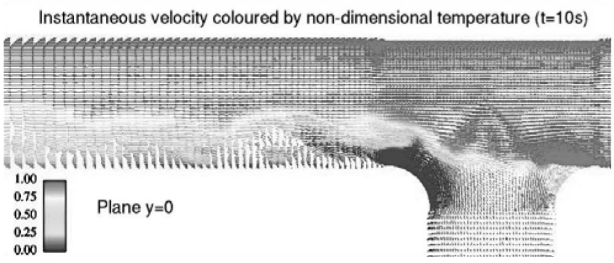

Fig. 6. Instantaneous Velocity Field in the Symmetry Plane, Coloured by the Non-dimensional Temperature, at Time t=10 s

[1] due to computing limitations, only 2 s of physical time have been simulated with the Smagorinsky model on the finer mesh

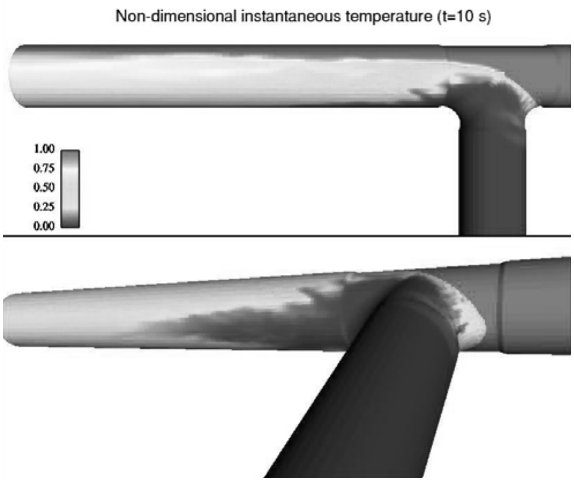

Fig. 7. Instantaneous Non-dimensional Temperature, at Time t=10 s

Figure 8 presents the mean velocity field in the symmetry plane and shows the recirculation downwind from the junction of the two branches. This recirculation reattaches around section C12.

Figures 9 and 10 respectively present the mean and the RMS temperature (obtained by time averaging of the instantaneous temperature field). Figure 11 shows the instantaneous temperature in the solid, at time t=10 s. It is clear that the field is much smoother than in the fluid (cf. Fig. 7), because of the strong attenuation due to the thermal inertia of the wall.

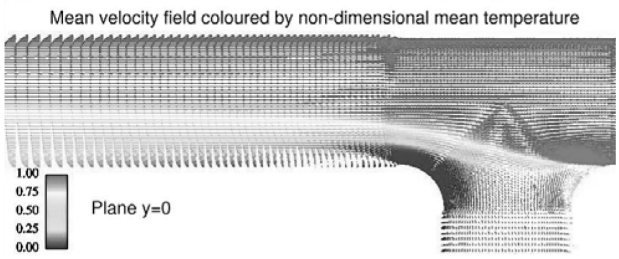

Fig. 8. : Mean Velocity Field in the Symmetry Plane, Coloured by the Mean Non-dimensional Temperature

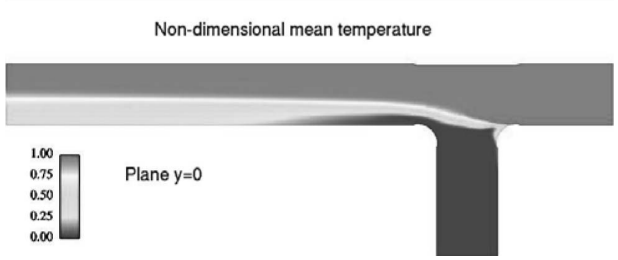

Fig. 9. Mean Non-dimensional Temperature in the Symmetry Plane

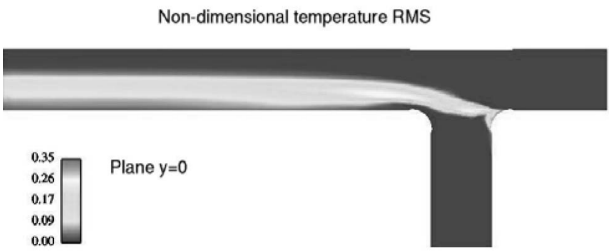

Fig. 10. Non-dimensional Temperature RMS in the Symmetry Plane

4.1 Temperature Evolution at the Fluid/Solid Interface

The focus is put on points located at the fluid/solid interface, corresponding to experimental probes on the mock-up. Figures 12 and 13 point out, on the C12 ring, the strong attenuation of the temperature signal of the wall compared to the very fluctuating temperature signal of the fluid in the near wall region. The angular positions of the probes on the ring are 50 degrees for Figure 12 and 10 degrees for Figure 13 (cf. Fig. 5). These probes will be further referenced as C1250 and C1210. This attenuation is due to the thermal inertia of the wall and is strongly dependent on the frequency of the fluctuations. This dependence is naturally reproduced by our unsteady simulation, whereas it is totally unreachable through averaged R.A.N.S. based approaches. Also, these figures show the large difference in the the level of thermal fluctuations between probe C1210, located in the cold stratification, and probe C1250, closer to the hot/cold interface.

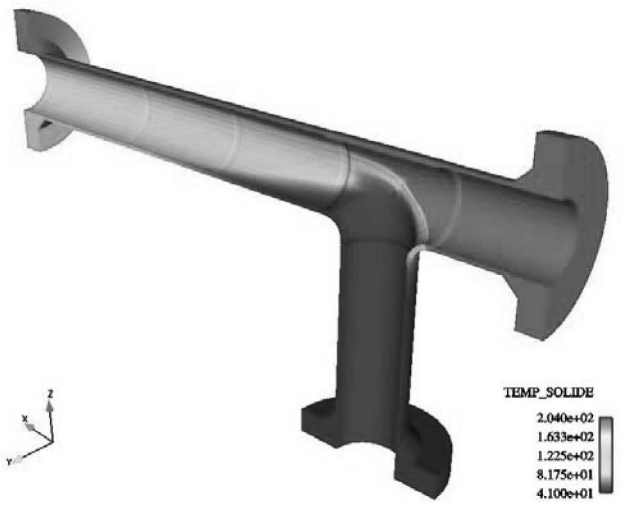

Fig. 11. Instantaneous Non-dimensional Temperature in the Solid at Time t=10 s

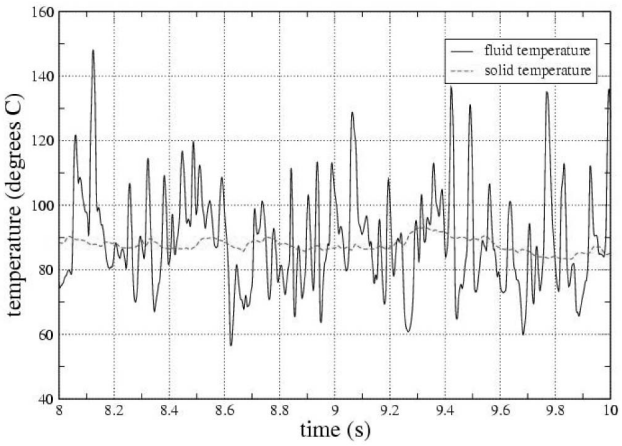

Fig. 12. Fluid and Solid Temperature at the Fluid/Solid Interface, Probe C1250

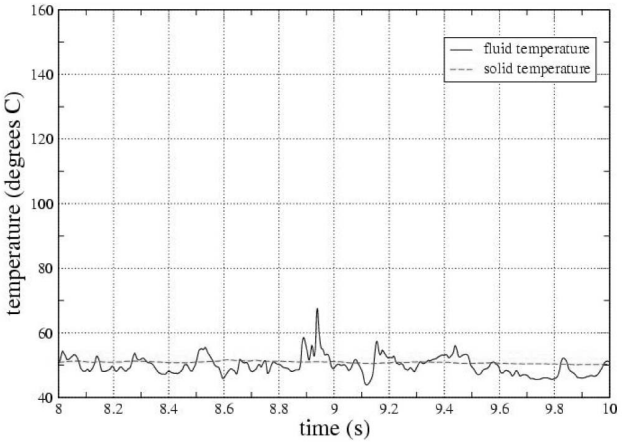

Fig. 13. Fluid and Solid Temperature at the Fluid/Solid Interface, Probe C1210

4.2 Temperature Evolution Within the Wall

As expected, the temperature fluctuation are extremely attenuated as soon as one considers points located further inside the wall. To give an overview, Figure 14 presents the RMS temperature decrease through the wall for probes on ring C25 at angle 50 degrees. This confirms the importance of solid mesh refinement at the fluid/solid interface.

5. COMPARISON WITH EXPERIMENTAL DATA

The results of our simulations will now be compared to experimental data taken from mock-up measurements.

5.1 Mean Temperature Along Measurement Rings

Figures 15 and 16 show the comparisons between the measurements and the three simulations for the non-dimensionnal temperature in the fluid, at the wall on rings C12 and C24. The sensitivity of the mesh refinement and of the subgrid scale model can clearly be seen. Indeed, on the finer mesh, the Smagorinsky model yields correct results on ring C12, but the comparison deteriorates along the flow, probably because of the the known difficulty of LES models to capture reattaching flows. On the coarser mesh, the Smagorinsky model yields a larger error close to the junction, but the comparison is strangely better towards ring C24. This might be due to error compensations rather than proper increase in precision. The third calculation, with the dynamic model, was proposed to try and get proper results at the junction that would not deteriorated after reattachment. Indeed it does give a more uniform behaviour, with proper comparison with the measurement all along the flow on the side of the pipe. Yet, there is a definite overestimation of the temperature on the lower pat of the sections (angle=0).

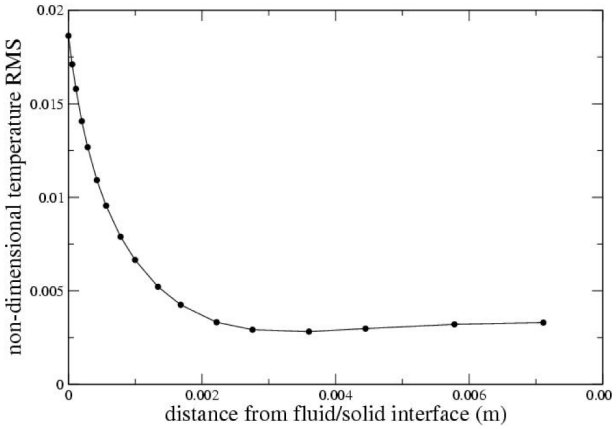

Fig. 14. Attenuation of the Non-dimensional Temperature RMS Through the Wall Thickness

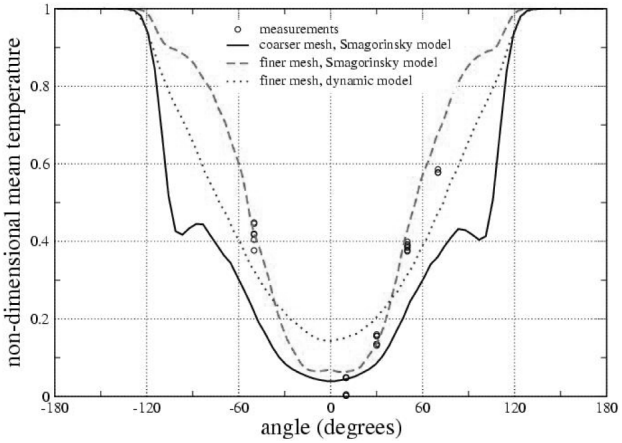

Fig. 15. Mean Fluid Non-dimensional Temperature Profile at the Wall on Ring C12

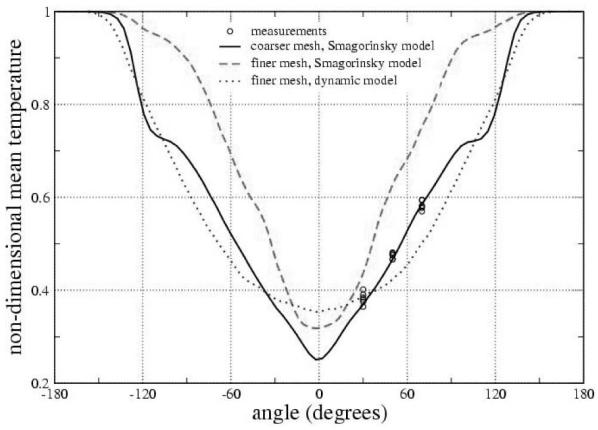

Fig. 16. Mean Fluid Non-dimensional Temperature Profile at the Wall on Ring C24

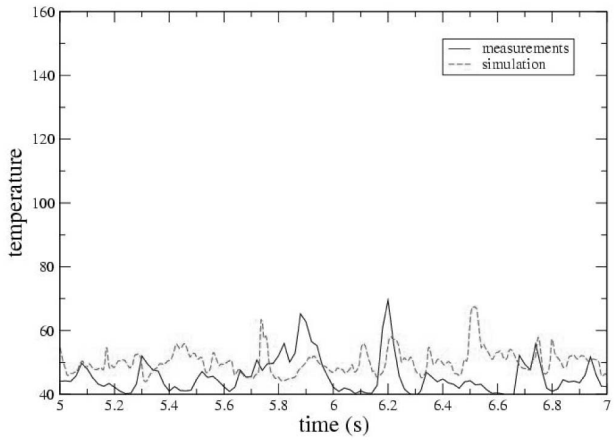

Fig. 18. Comparison Between Measurements and Simulation Results for the Instantaneous Fluid Temperature at Probe C1210

5.2 Time Evolution and Spectral Analysis

Figures 17 and 18 show the evolution of the instantaneous temperature in the fluid at probes C1250 and C1210, over 2 seconds of physical time, taken from experimental data and from the simulation. It shows reasonable agreement between both as far as the temperature RMS and frequencies are concerned. It should be noted that the sampling rate is much larger in the simulation. This is especially visible on probe C1250 (Figure 17). Results with the dynamic model are not shown here. They largely overestimate the temperature fluctuations at the wall.

Figures 19 and 20 show the evolution of the instantaneous temperature in the solid at probes C1250 and C1210, over 10 seconds of physical time, taken from experimental data and from the simulation. If results at probe C1250 still show reasonable agreement, it is not the case at probe C1210, where the simulation greatly underestimates the temperature fluctuations. Since the fluctuations in the fluid are correctly simulated (Fig. 18), it shows that the error originates in the

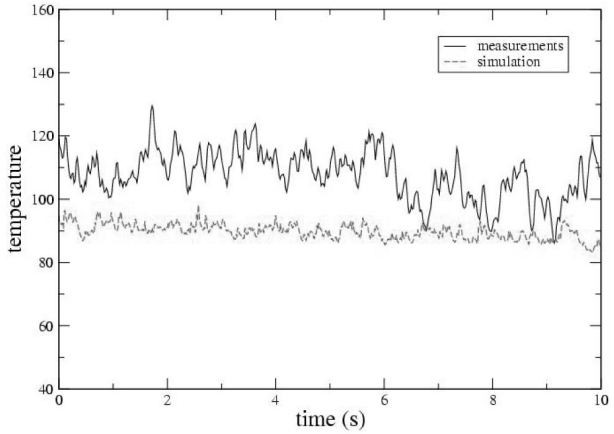

Fig. 19. Comparison Between Measurements and Simulation Results for the Instantaneous Solid Temperature at Probe C1250

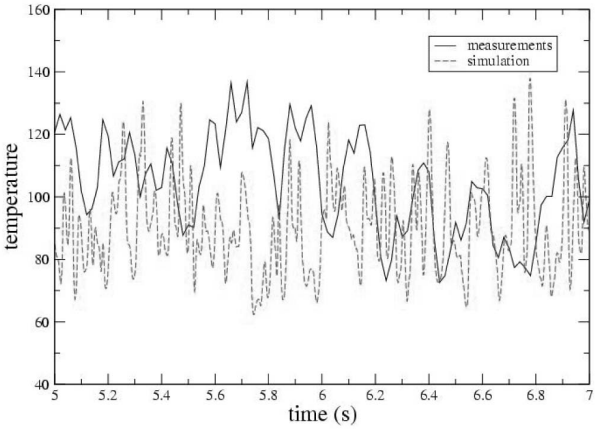

Fig. 17. Comparison Between Measurements and Simulation Results for the Instantaneous Fluid Temperature at Probe C1250

treatment of the fluid/solid interaction. Indeed the use of wall functions is not so appropriate for LES computations, and especially in the area of probe C1210, which corresponds the reattachment point at the end of the recirculation.

These results are corroborated by Figures 21 and 22 which show the Power Spectral Density Function for the solid temperature at probes C1250 and C1210. Reasonable agreement is shown on probe C1250, while large underestimation of temperature RMS is predicted at probe C1210.

6. CONCLUSION AND PERSPECTIVES

This paper presents a numerical approach able to address thermal fatigue problems occuring in pipeworks and its application to the simulation of a T-junction mock-up. A Large Eddy Simulation turbulent model implemented in EDF's CFD tool *Code_Saturne* yields instantaneous velocity and temperature fields. The thermal coupling with the finite element thermal code Syrthes allows to have access to the

instantaneous thermal field inside the wall. These solid thermal fields can then exploited with a mechanical tool to obtain thermally induced stresses. Different meshes and subgrid-scale models (Smagorinsky and dynamic) have been used on this study. As far as the fluid temperature is concerned, the simulation results compare farely well with the mock-up measurements. The Smagorinsky model shows difficulties dealing with the reattachment after the recirculation. The dynamic model shows a more uniform behaviour, but largely overestimates the temperature fluctuations at the wall and the temperature in the lower part of the mixing branch.

At the fluid/solid interface, heat transfer from the fluid to the wall is taken into account by standard wall functions. Although they seem to work quite well in some parts of the flow, they strongly overestimate the attenuation of the temperature fluctuations at the fluid/solid transfer in specific areas, like the recirculation zone, leading to a large error in solid temperature fluctuations.

Therefore, further efforts and theoretical developments are still needed for the subgrid-scale model and the near wall modelling. Also, although this methodology seems promising and is becoming more and more affordable as computer power increases, it is still very costly in terms of CPU time and computing memory.

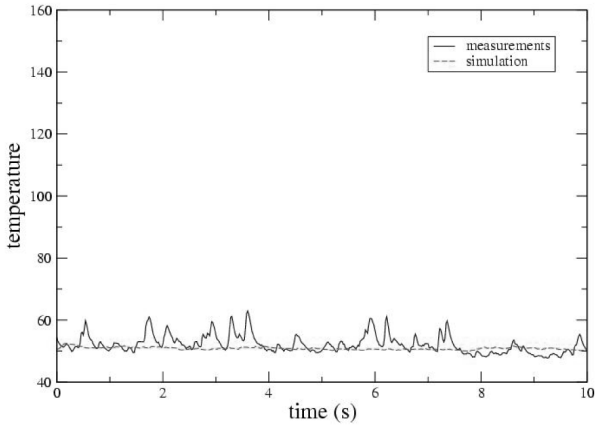

Fig. 20. Comparison Between Measurements and Simulation Results for the Instantaneous Solid Temperature at Probe C1250

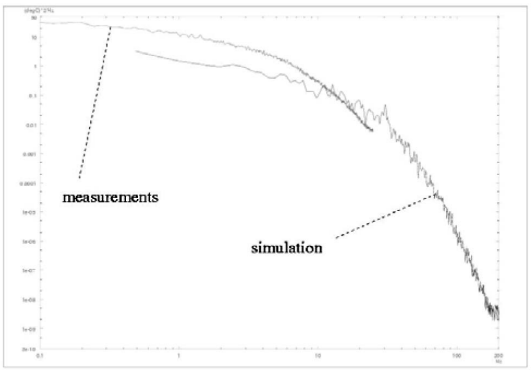

Fig. 21. Power Spectral Density Function for Solid Temperature at Probe C1250

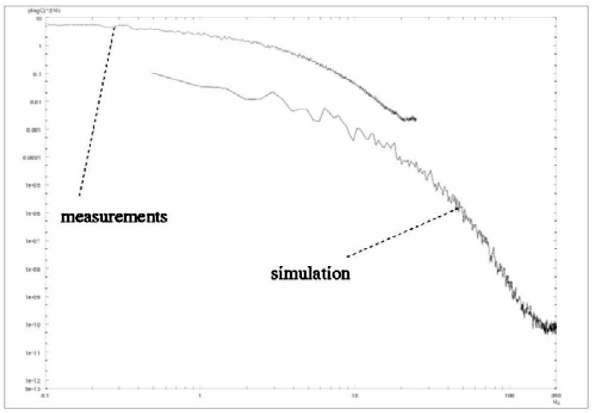

Fig. 22. Power Spectral Density Function for Solid Temperature at Probe C1210

REFERENCES

[1] J.M. Stephan, C. Peniguel, P. Genette, F. Curtit, M. Sakiz, Pasutto, S. Szaleniec, "Evaluation of Thermal Sollicitations and Stresses in Pipings Mixing Zones", Proceedings of ASME PVP05 Conference, Denver, Colorado, USA (2005).

[2] J. Smagorinsky, "General circulation experiments with the primitive equations, part I: the basic experiment", *Monthly Weather Rev*., **91**, 99-164 (1963).

[3] M. Germano, U. Piomlli, P. Moin, W.H. Cabot, "A dynamic subgrid scale eddy viscosity model", *Proceedings Summer Workshop*, Center for Turbulent Research, Stanford, California, USA (1990).

[4] S. Benhamadouche, D. Laurence, "LES, coarse LES and transient RANS comparisons on the flow across a tube bundle", *Proceedings of 5th Int Symp on Engineering Turbulence Modelling and Measurments*, W Rodi and N. Fueyo Edts, Elsevier, Mallorca, Spain (2002).

[5] S. Benhamadouche, K. Mahesh, G. Constantinescu, "Collocated Finite Volume Schemes for L.E.S. on Unstructured Meshes", *Proceeding of the 2002 Summer program*, Center for Turbulent Research, Stanford, California, USA (2002).

[6] C. Peniguel, M. Sakiz, S. Benhamadouche, J.M. Stephan, C. Vinderinho, "Presentation of a Numerical 3D Approach to Tackle Thermal Striping in PWR Nuclear T-Junction", ASME PVP Conference, Cleveland, USA (2003).

[7] J.H. Ferziger, M. Peric, *Computational Methods for Fluid Dynamics*, Springer, third edition (2002).

[8] C.M. Rhie, W.L. Chow, "A Numerical Study of a Turbulent Flow past an Isolated Airfoil with Trailing Edge Separation", *AIAA J*., **21**, 1525-1532 (1983).

[9] I. Rupp, C. Peniguel, "Coupling Heat Conduction, Radiation and Convection in Complex Geometries", *Int Journal of Numerical Methods for Heat and Fluid Flow*, **9** (1999).